

Dalton Transactions

Accepted Manuscript



This is an *Accepted Manuscript*, which has been through the Royal Society of Chemistry peer review process and has been accepted for publication.

Accepted Manuscripts are published online shortly after acceptance, before technical editing, formatting and proof reading. Using this free service, authors can make their results available to the community, in citable form, before we publish the edited article. We will replace this *Accepted Manuscript* with the edited and formatted *Advance Article* as soon as it is available.

You can find more information about *Accepted Manuscripts* in the [Information for Authors](#).

Please note that technical editing may introduce minor changes to the text and/or graphics, which may alter content. The journal's standard [Terms & Conditions](#) and the [Ethical guidelines](#) still apply. In no event shall the Royal Society of Chemistry be held responsible for any errors or omissions in this *Accepted Manuscript* or any consequences arising from the use of any information it contains.

Cite this: DOI: 10.1039/c0xx00000x

www.rsc.org/xxxxxx

ARTICLE TYPE

Uniform Iron Oxide Hollow Spheres for High-performance Delivery of Insoluble Anticancer Drugs

Yichen Zhu,^a Jie Lei,^{b*} Ye Tian^{a*}

Received (in XXX, XXX) Xth XXXXXXXXX 20XX, Accepted Xth XXXXXXXXX 20XX

DOI: 10.1039/b000000x

As an intrinsic character of many anticancer drugs, low solubility in physiological condition always limited the usage of these active ingredients in clinic. To overcome this bottleneck, we attempt to design and construct a high-performance magnetic-targeted delivery system based on uniform iron oxide hollow spheres. Via a facile one-pot solvothermal route, well-defined iron oxide hollow spheres were prepared with inexpensive inhesion. Compared with previously reported mesoporous Fe₃O₄ nanoparticles, our iron oxide hollow spheres with larger void space endowed the structures with high storage capacity of guest molecules. To confirm the efficiency of drug-loading and chemotherapy in vitro, camptothecin (CPT) was selected as a model insoluble anticancer drug in our present work. Detailed anticancer efficacy were further investigated by using MTT assays and microscope image method, indicating these iron oxide hollow spheres promising for insoluble drug delivery.

Introduction

Cancer has become the leading cause of death worldwide in accordance with the World Cancer Report.^{1, 2} Along with the rapid development of modern medicine, chemotherapy, surgery, and radiotherapy have been considered as main therapies and applied widely in clinic. However, low solubility of anticancer drug in physiological condition always limits their usages for efficient treatment in anticancer programs.³⁻⁶ For instance, intravenous administration of these insoluble chemical entities will form large aggregates in blood and induce serious side effect. More importantly, low solubility will cause insufficient drug accumulation around tumour sites and weaken chemotherapeutic efficiency.⁷

Recently, significant progress has been made to design novel drug delivery system (DDS) to enhance the bioavailability of hydrophobic drugs.⁸⁻¹³ Towards this goal, various micro/nano carriers including mesoporous particles, liposomes, and micelles have been constructed and applied for anticancer therapy by taking advantages of their rational biodistribution, minimal toxicity upon normal tissues, ease of surface functionality, as well as active target ability.¹⁴⁻²⁰ Among all these biomedicine materials, magnetic nanostructures have achieved much more attentions because of their potential applications in hyperthermia therapy, pre-clinical contrast agents, magnetic separation of biomolecules, as well as targeted drug delivery.²¹⁻³⁰ Compared with other magnetic materials, nanoparticles based on iron oxide

have been investigated the most owing to their chemical stability in physiological environment and high magnetic saturation.³¹⁻³⁵ For example, nanoballs containing Fe₃O₄ particles has been applied as FDA-approved magnetic resonance imaging contrast agents. Moreover, considerable approaches have been presented by integrating several advantages within one material for both diagnosis and therapy.³⁶⁻³⁸ In Addition, particles containing magnetic section and mesoporous section have also been well-prepared by several groups.³⁹⁻⁴³ Although promising, disadvantages, such as limited drug storage efficacy, poor response towards assistant magnet, and time-consuming synthesis still hamper these materials to be high-performance carriers in biomedicine applications. Thereby, the development of magnetic nanocarriers via a facile route, excellent internality, and high drug-loading capability is still urgently needed.

Current studies have demonstrated the preparation of various magnetic hollow structures, which extremely aroused extensive interest in fields of high drug-loading delivery systems.^{5,41} Inspired by these previous reports, herein, water-stable magnetic hollow spheres based on iron oxide were synthesized via a facile strategy, which could acted as a high-performance delivery platform for insoluble anticancer drugs. Fig. 1 illustrated the one-pot fabrication approach of our well-designed magnetic hollow spheres and their usage as drug-carriers to chemotherapeutics. Detailed solvent effect in solvothermal process was discussed, indicating the important role of ETA during the conformation course of hollow structure. In vitro toxicity studies promised their superior biocompatibility and neglectable cytotoxicity of magnetic hollow spheres. As a routinely used hydrophobic drug in clinic, camptothecin was selected to investigate the drug delivery efficiency, the drug release properties, as well as the anticancer effectiveness upon 786-O cells. Taking together, results obtained

^a Department of Urology, Beijing Friendship Hospital, Capital Medical University, Beijing, 100069 (P. R. China). E-mail: tianyebfh@gmail.com

^b Department of MRI, Fourth Hospital of Jilin University, Changchun, 130011 (P. R. China). E-mail: lei_jie_1@hotmail.com

†Electronic Supplementary Information (ESI) available: supporting figures. See DOI: 10.1039/b000000x/.

from our present work indicated that CPT-magnetic hollow spheres showed a high drug-loading capacity, nearly zero-release property in extracellular condition and high anticancer efficiency.

Materials and methods

Materials

Ferric chloride hexahydrate ($\text{FeCl}_3 \cdot 6\text{H}_2\text{O}$), anhydrous sodium acetate (NaOAc), polyethylene glycolethylene (PEG-2000), glycol (EG), ethanolamine (ETA), and ethanol were purchased from Beijing Chemicals. Camptothecin (CPT) was purchased from Aladdin Reagent. All chemical agents used in these experiments were of analytical grade and used directly without further purification.

Preparation of Fe_3O_4 hollow spheres

The monodisperse Fe_3O_4 hollow spheres were synthesized by one-pot solvothermal method. In detail, 1.5 g of $\text{FeCl}_3 \cdot 6\text{H}_2\text{O}$ was dissolved in 40 ml of solvent containing EG (30 mL) and ETA (10 mL) to form a stable orange solution. 4.0 g of NaAc and 1.0 g PEG-2000 were added into the above solution under vigorously magnetic stirring until completely dissolved. The obtained homogeneous solution was transferred to a Teflon-lined stainless-steel autoclave (50 mL) and sealed to heat at 200 °C. After reaction for 8 h, the autoclave was cooled to ambient temperature naturally. The obtained magnetite particles were washed with ethanol and deionized water in sequence, and then dried in vacuum at 60 °C for 12 h. With different amount of EG and ETA, solvent effect of ETA in solvothermal process was investigated in detail.

Loading of CPT and in vitro drug release

Camptothecin (CPT) loading was achieved by incubating CPT with Fe_3O_4 hollow spheres. Firstly, CPT powder was first dissolved in chloroform, making a saturated CPT solution at a concentration of 4 mg mL^{-1} . Above solution mixed with Fe_3O_4 hollow spheres (10 mg) was placed under stirring for 24 h. In this condition, Fe_3O_4 hollow spheres were filled with CPT. Then, the drug-loaded spheres were centrifuged, wash with PBS several times, and dried under vacuum at 70 °C overnight. The supernatant and washed solutions were collected and the residual drug content was determined by UV-vis method to calculate the drug-loading capacity of Fe_3O_4 hollow spheres. In vitro release experiments were performed under different solvent conditions. Detailedly, 1 mg of CPT- Fe_3O_4 were resuspended in a centrifuge tube (10 mL) containing 5 mL PBS or DMSO. At certain time intervals, Fe_3O_4 hollow spheres were centrifuged, and 0.5 mL release medium containing the free drug was transferred out to determine the concentration of CPT.

Cell cultures

786-O cells (human kidney carcinoma cell line), NIH3T3 cells (mouse embryonic fibroblast cell line), HepG2 cells, and Hela cells were supplied by American Type Culture Collection. 786-O cells were cultured in 1640 medium containing penicillin (100 U mL^{-1}), streptomycin (100 U mL^{-1}), and 10% fetal bovine serum (FBS) in a humidified incubator at 37 °C and 5% CO_2 . NIH3T3 cells were cultured in DMEM containing penicillin (100 U mL^{-1}),

streptomycin (100 U mL^{-1}), and 10% fetal bovine serum (FBS) in a humidified incubator at 37 °C and 5% CO_2 . Both cells were harvested by the use of trypsin and were resuspended in fresh complete medium before plating.

In vitro cytotoxicity studies

MTT assays were performed to quantify the cytotoxicity of Fe_3O_4 hollow spheres. Typically, 786-O cells and NIH3T3 cells were cultured in 96-well plates with a density of 5×10^3 per well for 12 h to allow the cells to attach. Serial dilutions of different formulations containing Fe_3O_4 hollow spheres were added to the culture medium. At the end of the incubation time, medium containing Fe_3O_4 hollow spheres were removed, and cell samples were treated with MTT for another 4 h, which was followed by the addition of DMSO to dissolve the formazan crystals. Bio-Rad model-680 microplate reader was applied to measure the absorbance at a wavelength of 570 nm. Six replicates were done for each treatment group and percent viability was normalized to cell viability in the absence of Fe_3O_4 hollow spheres.

In vitro anticancer activity

MTT assays were further carried out to evaluate the cytotoxicity of CPT- Fe_3O_4 . Briefly, 786-O cells, HepG2 cells, and Hela cells were respectively seeded in 96-well plates with a density of 5×10^3 per well for 12 h to allow the cells to attach. CPT and CPT- Fe_3O_4 with expected formulations were added to the medium. Cells were incubated in 5% CO_2 at 37 °C for 24 h. At the end of incubation time, cell samples were treated via MTT assay.

Cellular modality and observation

For microscope imaging, 786-O cells with a density of 2×10^4 were plated in a 24-well plate for 4 h to allow the cells to attach. After the cells were washed twice by cool phosphate-buffered saline (PBS), Fe_3O_4 hollow spheres, CPT, and CPT- Fe_3O_4 with a concentration of 25 $\mu\text{g mL}^{-1}$ were added to the culture medium. After incubating for 24 h, cells were washed again with PBS several times to remove the remaining nanoparticles. In order to nucleus labeling, nuclei was stained with Hoechst 33342 (20 mg mL^{-1} in PBS) for 10 min, rinsed with PBS, and then observed under an Olympus BX-51 optical system microscopy. In addition, 786-O cells were stained with trypan blue for 15 min, washed with PBS, and then imaged by a digital microscope. Pictures were then taken with an Olympus digital camera.

Detection of Fe^{3+} in 786-O cells

To detection the amount of Fe^{3+} in cells, 786-O cells were plated in a 24-well plate for 4 h to allow the cells to attach. Then, Fe_3O_4 hollow spheres and CPT- Fe_3O_4 were added to the culture medium with a concentration of 25 $\mu\text{g mL}^{-1}$ (1mL). After 24 h incubation, cells were washed with PBS several times to remove the remaining nanoparticles. Then concentrated HCl was added to above systems to obtain cell lysis for ICP-MS analysis.

Statistical analysis

All data were expressed in this article as mean result \pm standard deviation (SD). The statistical analysis was performed by using Origin 8.0 software.

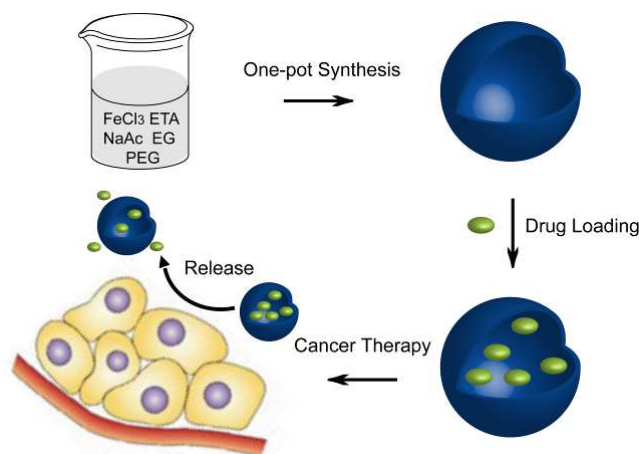


Fig. 1 Schematic illustration of one-pot synthesis of Fe_3O_4 hollow spheres and their applications to chemotherapeutics.

Results and discussion

The synthesis of uniform magnetic hollow spheres was carried out using a modified facile solvothermal method.³¹ Detailed morphological and structural features of Fe_3O_4 hollow spheres were examined via scanning electron microscopy (SEM) and transmission electron microscopy (TEM) at first. As exhibited in Fig. 2A, Fig. 2B, and Fig. S1, Fe_3O_4 hollow spheres with uniform and non-aggregated nature revealed a relatively coarse surface and a mean diameter of ~ 200 nm, which were composed of small primary nanoparticles with an average size of 30-40 nm. The roughness of surface should be attributed to the accumulation effect of small nanocrystals. Careful observation of a single hollow sphere based on high-magnification SEM image shown in Fig. 2A additionally revealed that the magnetic hollow sphere was constructed of smaller nanocrystals. As illustrated in Fig. 2C, wide-angle XRD pattern of the magnetic hollow spheres revealed

the characteristic broad diffraction peaks of well-defined magnetite phase (JCPDS 75-1609). As shown in Fig. 2D, EDS results originated from point scan indicated that the sample mainly contained Fe and O elements. The graft of PEG molecules on nanocarriers could extremely enhance their biocompatibility, monodispersity, and hydrophilicity.⁴⁴⁻⁴⁶ In our present work, PEG-2000 was introduced and applied to form PEG-modified magnetic hollow spheres. Based on our thermogravimetric analysis (TGA) result, the content of PEG molecules was calculated to be 7.21% (Fig. S2). Multifunctional nanomaterials with excellent response towards assistant magnet have gained much attention due to their unique magnetic-separable and magnetic-targeted features.⁴⁷⁻⁵⁰ As illustrated in Fig. 2E, the magnetic property collected on a SQUID magnetometer at room temperature demonstrated the magnetization saturation value of Fe_3O_4 hollow spheres was 82.67 emu g^{-1} . Photograph shown in Fig. 2F revealed an admirable dissolution and a visible response of the as-prepared hollow spheres towards an appropriate magnet. The nitrogen absorption/desorption isotherms of our magnetic hollow spheres was illustrated in Fig. S3. It could be seen that the sample exhibited typical IV-typed isotherms with H1-hysteresis loops, indicating the presence of mesopores. BET surface area and total pore volume were calculated to be $15.23 \text{ m}^2 \text{ g}^{-1}$ and $0.174 \text{ cm}^3 \text{ g}^{-1}$, respectively. Dynamic light scattering (DLS) analysis of these Fe_3O_4 hollow spheres in PBS containing 10% FBS illustrated an average diameter of 224 nm, which was larger than that of TEM observation and thus indicated the successful modification of PEG molecules on the surface of the spheres. Otherwise, the zeta potential of these Fe_3O_4 hollow spheres was -2.41 mV . To sum up, these well-defined Fe_3O_4 hollow spheres promised more potential for biomedicine applications.

To investigate the solvent effect of ETA in the formation process, control experiments were carried out additionally. As illustrated in Fig. 3A, no hollow structures were obtained except for solid magnetic nanoparticles. When the amount of ETA was

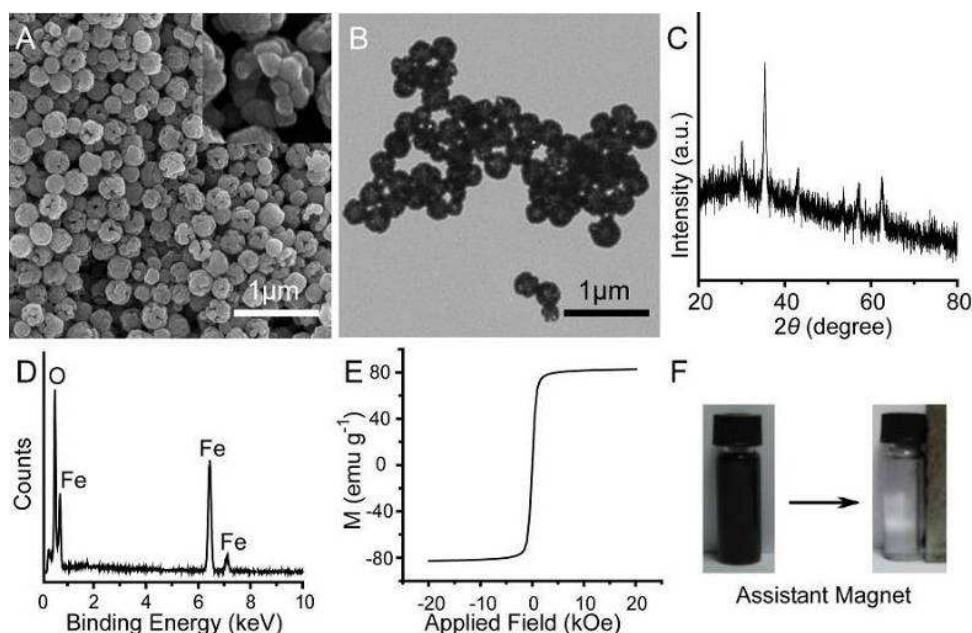


Fig. 2 SEM micrograph (a), TEM image (b), wide-angle XRD pattern (c), EDS spectrum (d), room-temperature field-dependent magnetization curve (e), as well as visible magnetic-response process (f) of Fe_3O_4 hollow spheres.

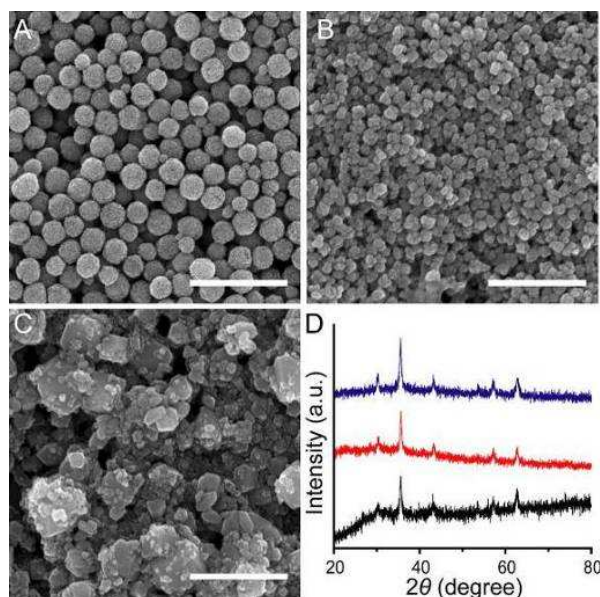


Fig. 3 SEM images and wide-angle XRD patterns (d) of Fe_3O_4 obtained upon different solvent conditions: without ETA (a and black), ETA:EG = 1:1 (band red), as well as ETA:EG = 3:1 (c and blue) (scale bar: 1 μm).

increased to half of the total, nanocrystal with an average size of 30 nm could be achieved (Fig. 3B). However, amorphous products with agglomerate magnetic materials were gained while ETA increased to three-quarter content (Fig. 3C). The formation mechanism of magnetic hollow spheres was attributed to the intense coordination between amido of ETA and Fe^{3+} . Complex composed with ETA and Fe^{3+} could limit the rapid growth of nanoparticles, resulting in the formation of smaller nanocrystals. Under proper solvent condition, smaller nanocrystals assembled into hollow spheres as expected. Wide-angle XRD patterns shown in Fig. 3D further indicated the magnetite phase of all these products.

Cell viability under the co-incubation with nanoparticles was evaluated at first to examine the feasibility of obtained magnetic hollow spheres in a drug delivery system. As shown in Fig. 4A, Fe_3O_4 hollow spheres did not present cytotoxicity against 786-O cells. Significantly, the cell viability still remained above 95% even under a high concentration of 200 $\mu\text{g mL}^{-1}$. Otherwise, we selected NIH3T3 cells (a normal cell line) to investigate the in vitro toxicity of magnetic hollow spheres. As illustrated in Fig. S4, cell viabilities were not hindered by Fe_3O_4 hollow spheres up to a concentration of 200 $\mu\text{g mL}^{-1}$. In addition, long-term dialysis against natural PBS containing 10% fetal bovine serum was performed to examine the stability of Fe_3O_4 hollow spheres in physiological condition. Result revealed that there was no leaching of free Fe^{3+} from the magnetic hollow spheres, indicating their excellent stability. However, when experiment was carried out under acid condition (pH = 4.5), result of the dialysis demonstrated the dissolution of Fe_3O_4 hollow spheres and the presence of Fe^{3+} achieved via ICP-MS method. On the basis of these results, it could be inferred that our magnetic nanocarriers decomposed during endocytosis, released drug in cytoplasm, and resulted in the high-performance cancer treatment. To date, lack of aqueous solubility always limited their

practical applications of many anticancer drugs in clinic.^{3,5,18} To overcome this bottleneck, hollow materials with large space for storing guest molecules held more potential for the development of novel delivery systems. With the unique hollow feature of our Fe_3O_4 particles, it was highly desired to apply Fe_3O_4 hollow structures as efficient nanocarriers of hydrophobic drugs in cancer therapy. Camptothecin (CPT) was employed as a model hydrophobic anticancer drug in our current study. The Fe_3O_4 hollow spheres were loaded with CPT molecules by soaking them in DMSO containing CPT 24 h. After CPT- Fe_3O_4 was removed via careful centrifugation, CPT- Fe_3O_4 was washed twice with PBS to confirm that there was no additional adsorbed drug on the surface of Fe_3O_4 hollow spheres. Detected via UV-vis method, approximate 120 μg of CPT molecules were stored inside 1 mg of hollow spheres, demonstrating the high loading capacity of Fe_3O_4 hollow spheres (Fig. S5). Fig. 4B revealed the released amounts of CPT when the CPT- Fe_3O_4 were dispersed in PBS (pH = 7.4) and DMSO with different incubation periods, respectively. Less than 3% of the stored CPT could be released into the supernatant when CPT- Fe_3O_4 was dispersed in PBS and left in suspension for up to 4 h. However, once CPT- Fe_3O_4 was dispersed in DMSO for 0.5 h, most of CPT could be released and detected in the supernatant. Above results suggested the negligible drug leakage in PBS of CPT- Fe_3O_4 and great significance in the minimization of side effects. Viabilities of 786-O cells against CPT and CPT- Fe_3O_4 after incubation for 24 h were present in Fig. 4C. Compared with control group, both CPT and CPT- Fe_3O_4 exhibited toxicity towards 786-O cells. Slight cytotoxicities of free CPT were probably in accordance with the low solubility of CPT in hydrophilic medium. Much higher cytotoxic efficacy of CPT- Fe_3O_4 further made out the efficient drug-delivery capability by using carriers. Due to the presence of hydrophobic sections in cells, CPT- Fe_3O_4 could rationally release CPT at these active sites, which played an important role to kill cancer cells. To confirm the internalization route of Fe_3O_4 hollow spheres and CPT- Fe_3O_4 composites, we investigated the amount of Fe^{3+} in 786-O cells via ICP-MS method. Nearly 70% of the initial Fe^{3+} content could be detected both in Fe_3O_4 and CPT- Fe_3O_4 groups (184 $\mu\text{g well}^{-1}$ for Fe_3O_4 and 176 $\mu\text{g well}^{-1}$ for CPT- Fe_3O_4), which indicated that the loading process of CPT presented no effect on the endocytosis of nanocarriers. To obtain a generalized conclusion, another two kinds of carcinoma cell lines including HepG2 cells and Hela cells were selected to investigate the delivery efficiency of Fe_3O_4 hollow spheres. As exhibited in Fig. S6, CPT- Fe_3O_4 could kill more cells than CPT only based on both mentioned cell lines, which foretold that the magnetic hollow spheres could act as high-performance carriers during the drug delivery system. In addition, morphological change of cell nuclei observed via fluorescence microscope imaging was investigated to provide a systemic explanation for above excellent anticancer efficiency. As shown in Fig. 4D, all the nuclei revealed normal morphology without any accumulation of chromatin, indicating our Fe_3O_4 showed nearly no toxicity towards cells. On the contrary, obvious nuclear fragmentation and accumulation of chromatin could occur in most of 786-O cells incubated upon CPT- Fe_3O_4 , while fewer condensed nuclei presented in 786-O cells incubated with CPT only. To further demonstrate the performance of Fe_3O_4 hollow spheres in drug delivery system,

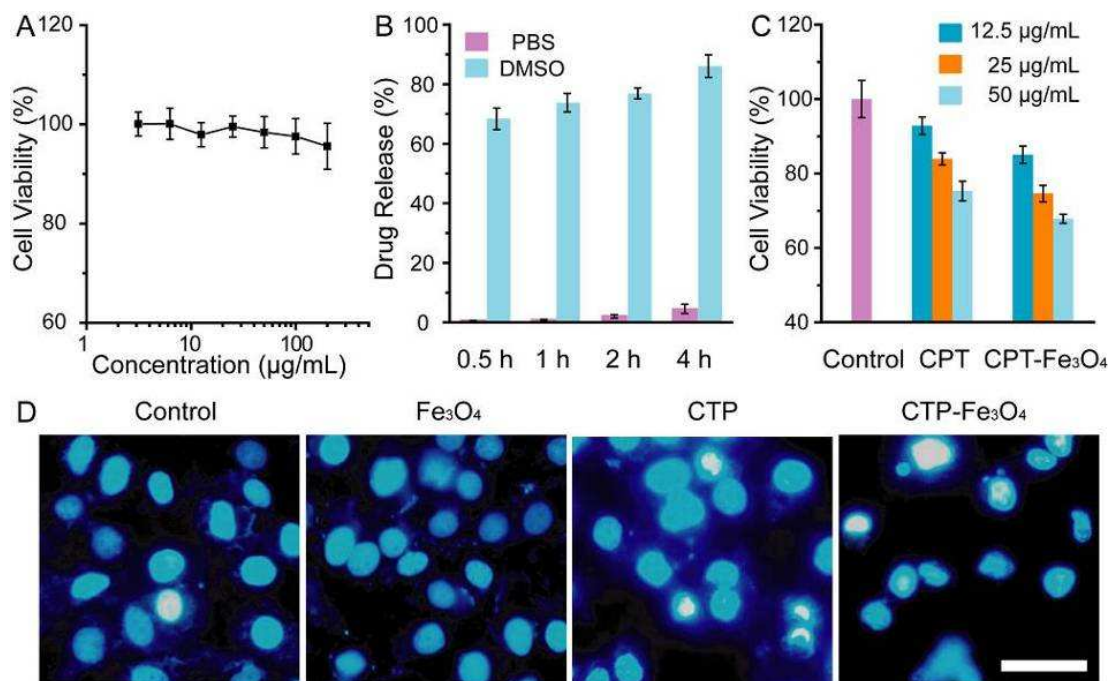


Fig. 4 Effect of Fe₃O₄ hollow spheres on the viability of 786-O cells under 24 h of incubation (a), release amounts of CPT from CPT-Fe₃O₄ complex measured via UV-vis method (b), viability of 786-O cells incubated with CPT and CPT-Fe₃O₄ upon different incubation concentrations (c), as well as microscope imaging photos of stained nuclei of 786-O cells (d) (scale bar: 50 μm).

tryblue staining shown in Fig. S7 also indicated our above description. There were more death occurred in CPT-Fe₃O₄ group than Fe₃O₄ group, indicating neglectable toxicity in vitro. Thus, it could be deduced that well-prepared Fe₃O₄ hollow spheres could potentially be applied as effective vehicles to store and deliver highly toxic and water-insoluble anticancer drug for cancer treatment.

Conclusions

In summary, monodisperse magnetic hollow spheres based on iron oxide with excellent magnetic response have been successfully designed and constructed via a facile one-pot solvothermal route. The amount of ETA in solvent played an important role during the formation of Fe₃O₄ hollow structure, indicating the solvent effect in preparation of nanomaterials. These well-prepared Fe₃O₄ hollow spheres could effectively deliver insoluble anticancer drug to the cancer cells due to the presence of large inner cavity. Otherwise, CPT-Fe₃O₄ composites demonstrated a much higher anticancer activity than single CPT in accordance with its low solubility in physiological condition. Above results indicated our magnetic hollow spheres promised the potentials in anticancer drug delivery and cancer treatment in vitro.

References

- R. Bardhan, S. Lal, A. Joshi, N. Halas, *Acc. Chem. Res.* 2011, **44**, 936.
- D. Yoo, J. Lee, T. Shin, J. Cheon, *Acc. Chem. Res.* 2011, **44**, 863.
- W. Wei, Z. Yue, J. Qu, H. Yue, Z. Su, G. Ma, *Nanomedicine* 2010, **5**, 589.

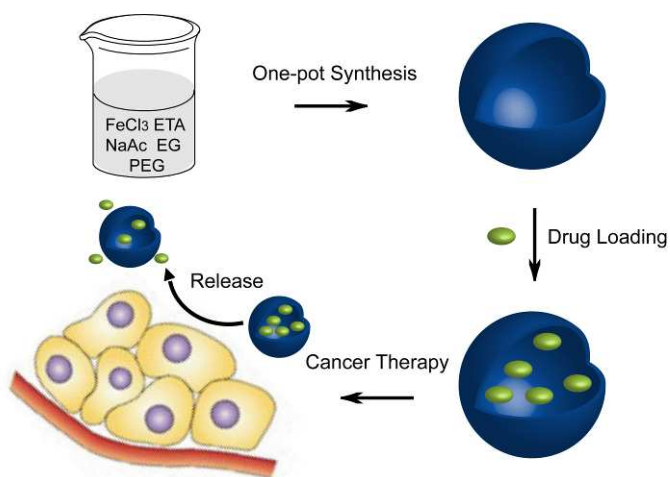
- C. Lipinski, *Am. Pharm. Rev.* 2002, **5**, 82.
- Z. Yue, W. Wei, Z. You, Q. Yang, H. Yue, Z. Su, G. Ma, *Adv. Funct. Mater.* 2011, **21**, 3446.
- F. Wischke, S. Schwendeman, *Int. J. Pharm.* 2008, **364**, 298.
- C. Lipinski, F. Lombardo, B. Dominy, P. Feeney, *Adv. Drug Deliv. Rev.* 2001, **46**, 3.
- B. Parakhonskiy, A. Haase, R. Antolini, *Angew. Chem. Int. Ed.* 2012, **51**, 1195.
- P. Yang, Z. Quan, C. Li, X. Kang, H. Lian, J. Lin, *Biomaterials* 2008, **29**, 4341.
- M. Melancon, A. Elliott, A. Shetty, Q. Huang, R. Stafford, C. Li, *J. Controlled Release* 2011, **156**, 265.
- W. Zhao, H. Chen, Y. Li, L. Li, M. Lang, J. Shi, *Adv. Funct. Mater.* 2008, **18**, 2780.
- Y. Zhu, T. Ikoma, N. Hanagata, S. Kaskel, *Small* 2010, **6**, 471.
- R. Hao, R. Xing, Z. Xu, Y. Hou, S. Gao, S. Sun, *Adv. Mater.* 2010, **22**, 2729.
- X. Lou, L. Archer, Z. Yang, *Adv. Mater.* 2008, **20**, 3987.
- D. Yang, X. Kang, P. Ma, Y. Dai, Z. Hou, Z. Cheng, C. Li, J. Lin, *Biomaterials* 2013, **34**, 1601.
- H. Liu, D. Chen, L. Lin, T. Liu, L. Tan, X. Wu, F. Tang, *Angew. Chem. Int. Ed.* 2011, **50**, 891.
- Y. Chen, H. Chen, J. Shi, *Acc. Chem. Res.* DOI: 10.1021/ar400091e
- Z. Liu, X. Liu, Q. Yuan, K. Dong, L. Jiang, Z. Li, J. Ren, X. Qu, *J. Mater. Chem.* 2012, **22**, 14982.
- S. Skrabalak, J. Chen, Y. Sun, X. Lu, L. Au, C. Cobley, Y. Xia, *Acc. Chem. Res.* 2008, **41**, 1587.
- M. Ambrogio, C. Thomas, Y. Zhao, J. Zink, J. Stoddart, *Acc. Chem. Res.* 2011, **44**, 903.
- W. Dong, Y. Li, D. Niu, Z. Ma, J. Gu, Y. Chen, W. Zhao, X. Liu, C. Liu, J. Shi, *Adv. Mater.* 2011, **23**, 5392.
- S. Selvan, P. Patra, C. Ang, J. Ying, *Angew. Chem. Int. Ed.* 2007, **46**, 2448.
- J. Ge, Q. Zhang, T. Zhang, Y. Yin, *Angew. Chem. Int. Ed.* 2008, **47**, 8924.
- H. Wu, S. Zhang, J. Zhang, G. Liu, J. Shi, L. Zhang, X. Cui, M. Ruan, Q. He, W. Bu, *Adv. Funct. Mater.* 2011, **21**, 1850.

- 25 B. Kim, N. Lee, H. Kim, K. An, Y. Park, Y. Choi, K. Shin, Y. Lee, S. Kwon, H. Na, J. Park, T. Ahn, Y. Kim, W. Moon, S. Choi, T. Hyeon, *J. Am. Chem. Soc.* 2011, **133**, 12624.
- 26 N. Frey, S. Peng, K. Cheng, S. Sun, *Chem. Soc. Rev.* 2009, **38**, 2532.
- 5 27 C. Xu, Z. Yuan, N. Kohler, J. Kim, M. Chung, S. Sun, *J. Am. Chem. Soc.* 2009, **131**, 15346.
- 28 Z. Liu, M. Li, X. Yang, M. Yin, J. Ren, X. Qu, *Biomaterials* 2011, **32**, 4683.
- 10 29 W. Seo, J. Lee, X. Sun, Y. Suzuki, D. Mann, Z. Liu, M. Terashima, P. Yang, M. McConnell, D. Nishimura, H. Dai, *Nat. Mater.* 2006, **5**, 971.
- 30 K. Yan, H. Li, P. Li, H. Zhu, J. Shen, C. Yi, S. Wu, K. Yeung, Z. Xu, H. Xu, P. Chu, *Biomaterials* 2014, **35**, 344.
- 15 31 H. Deng, X. Li, Q. Peng, X. Wang, J. Chen, Y. Li, *Angew. Chem. Int. Ed.* 2005, **44**, 2782.
- 32 W. Cheng, K. Tang, J. Sheng, *Chem. Eur. J.* 2010, **16**, 3608.
- 33 P. Yang, Z. Quan, Z. Hou, C. Li, X. Kang, Z. Cheng, J. Lin, *Biomaterials* 2009, 4786.
- 20 34 W. Ma, Y. Zhang, L. Li, L. You, P. Zhang, Y. Zhang, J. Li, M. Yu, J. Guo, H. Lu, C. Wang, *ACS Nano* 2012, **6**, 3179.
- 35 S. Liu, H. Chen, X. Lu, C. Deng, X. Zhang, P. Yang, *Angew. Chem. Int. Ed.* 2010, **49**, 7557.
- 36 J. Kim, H. Kim, N. Lee, T. Kim, H. Kim, T. Yu, I. Song, W. Moon, T. Hyeon, *Angew. Chem. Int. Ed.* 2008, **47**, 8438.
- 25 37 J. Choi, Y. Jun, S. Yeon, H. Kim, J. Shin, J. Cheon, *J. Am. Chem. Soc.* 2006, **128**, 15982.
- 38 M. Liong, J. Lu, M. Kovichich, T. Xia, S. Ruehm, A. Nel, F. Tamanoi, J. Zink, *ACS Nano* 2008, **2**, 889.
- 30 39 C. Thomas, D. Ferris, J. Lee, E. Choi, M. Cho, E. Kim, J. Stoddart, J. Shin, J. Cheon, J. Zink, *J. Am. Chem. Soc.* 2010, **132**, 10623.
- 40 Y. Zhao, L. Lin, Y. Lu, H. Gao, S. Chen, P. Yang, S. Yu, *Adv. Healthcare Mater.* 2012, **1**, 327.
- 41 X. Kang, Y. dai, P. Ma, D. Yang, C. Li, Z. Hou, Z. Cheng, J. Lin, *Chem. Eur. J.* 2012, **18**, 15676.
- 35 42 S. Guo, D. Li, L. Zhang, J. Li, E. Wang, *Biomaterials* 2009, **30**, 1881.
- 43 F. Wang, X. Chen, Z. Zhao, S. Tang, X. Huang, C. Lin, C. Cai, N. Zheng, *J. Mater. Chem.* 2011, **21**, 11244.
- 40 44 M. Zhu, G. Nie, H. Meng, T. Xia, A. Nel, Y. Zhao, *Acc. Chem. Res.* 2013, **46**, 622.
- 45 Z. Liu, J. Robinson, X. Sun, H. Dai, *J. Am. Chem. Soc.* 2008, **130**, 10876.
- 46 Z. Liu, F. Pu, S. Huang, Q. Yuan, J. Ren, X. Qu, *Biomaterials* 2013, **34**, 1712.
- 45 47 Y. Jun, J. Seo, J. Cheon, *Acc. Chem. Res.* 2008, **41**, 179.
- 48 S. Hu, K. Kuo, W. Tung, D. Liu, S. Chen, *Adv. Funct. Mater.* 2009, **19**, 3396.
- 49 C. Xu, K. Xu, H. Gu, R. Zheng, H. Liu, X. Zhang, Z. Guo, B. Xu, *J. Am. Chem. Soc.* 2004, **126**, 9938.
- 50 50 S. Gai, P. Yang, C. Li, W. Wang, Y. Dai, N. Niu, J. Lin, *Adv. Funct. Mater.* 2010, **20**, 1166.

Table of Contents

Uniform Iron Oxide Hollow Spheres for High-performance Delivery of Insoluble Anticancer

Drugs



5

Novel magnetic hollow spheres based on iron oxide have been designed and synthesized via a facile and cost-effective one-pot solvothermal route, which successfully acted as nanocarriers for the high-performance delivery of insoluble anticancer drugs *in vitro*.